



## A Simple Approach to Predict the Shear Capacity and Failure Mode of Fix-ended Reinforced Concrete Deep Beams based on Experimental Study

A. Arabzadeh\*, R. Hizaji

Department of Civil Engineering, Tarbiat Modares University, Tehran, Iran

### PAPER INFO

#### Paper history:

Received 07 January 2019

Received in revised form 23 January 2019

Accepted 07 March 2019

#### Keywords:

Fix-ended Deep Beam

Strut and Tie Model

Shear Failure

Cyclic Load

### ABSTRACT

Reinforced Concrete (RC) deep beams are commonly used in structural design to transfer vertical loads when there is a vertical discontinuity in the load path. Due to their deep geometry, the force distribution within the RC deep beams is very different than the RC shallow beams. There are some strut and tie model (STM) already been developed for RC deep beams. However, most of these models are developed for RC deep beams with the simply supported boundary condition, which do not apply for RC deep beams with the fix-ended condition. In this paper, five fixed-end RC deep beams have been tested experimentally which were subjected to monotonic and cyclic loads. Also, a simple STM was proposed to simulate the load capacity and failure mode of fix-ended RC deep beams. The proposed STM has the main strut and sub struts to simulate the force distribution within the RC deep beams. This STM were verified using five fixed-end RC deep beams subjected to monotonic and cyclic loads and compared to the response of 31 additional independent experimental tests. The result shows the newly proposed STM can simulate the load capacity and failure mode of fix-ended RC deep beams very well.

doi: 10.5829/ije.2019.32.04.a.03

## 1. INTRODUCTION

Fix-ended reinforced concrete (RC) deep beams are fairly common structural elements. They are used as load distribution elements such as transfer girders, pile caps, and foundation walls, often receiving many small loads and transferring them to two supports. Fix-ended RC deep beams differ from either simply supported reinforced concrete deep beams or continuous reinforced concrete shallow beams. In fix-ended deep beams, the regions of high shear and high moment coincide and failure usually occurs in these regions. The classical elastic theory of bending is not valid in these regions, and the design of the deep beams is intended to consider the shear effect. The load carrying capacity of a deep beam depends on the strength of the compressive strut that joins the loading point and the support reaction point [1]. In simply supported deep beams, the region of high shear coincides with the region of a low moment.

\*Corresponding Author Email: [arabzade@modares.ac.ir](mailto:arabzade@modares.ac.ir) (A. Arabzadeh)

The failure mechanisms of fix-ended and simply supported deep beams are different. Despite the different failure mechanisms, the current design codes of practice for shear in fix-ended RC deep beams are based entirely on tests of simply supported deep beams because there have not been theoretical and experimental studies on fix-ended deep beams [2]. Because creating the fixity of supports is difficult in the laboratory [3, 4].

One of the most crucial failures in RC deep beams is the shear failure [5]. Failure due to the shear in reinforced concrete elements is brittle and occurs suddenly without warning. Several researchers have investigated experimentally and analytically to evaluate shear carrying capacity of reinforced concrete members [6, 7]. It has been found that several mechanisms including the shear transfer in the compression zone, aggregate interlock across the crack face, stirrups crossing the shear crack, and dowel action of longitudinal reinforcing bars crossing the crack can be involved to provide shear resistance of reinforced concrete (RC) beams [8].

Regarding recent tendency for application of deep beams, possibility of using fixed-ended deep beams has been widely increased in structures. Therefore, it seems necessary to investigate aforementioned structural element in more details. Due to probable architectural requirements of columns elimination or structural failure of them, this kind of beams may be suffered of cyclic loads during earthquakes.

The Strut-Tie Model (STM) approach, known as a design method for structural concrete with disturbed regions, has been accepted in the current design codes including the BS8110 [9], CSA [10], FIB [11], AASTHO-LRFD [12] and ACI 318M-14 [13]. The approach has mainly been applied to the analysis and shear design of simply supported reinforced and prestressed concrete deep beams [14-17]. However, even though excluding the subject of continuous deep beams, an appropriate strut-tie model that represents a true load transfer mechanism for simply supported deep beams. The model and reflects the effects of the primary design variables on shear behavior which is provided. Though the studies about the strut-tie model analysis and design of continuous deep beams were conducted by Alshegeir [18] and MacGregor [19]. A simple determinate truss type of strut-tie model which seems to be incapable of representing appropriate load transfer mechanisms of continuous deep beams was presented. Arabzadeh [20] proposed the STM model to analyze fix-ended RC deep beams under monotonic loads. The proposed model was verified using 18 fix-ended RC deep beams experimental tests [3]. Similarly, Hwang et al. [21] also proposed novel STM to predict the shear strength of squat RC walls. Also, Kassem [22] proposed a closed form for the design of squat walls according to Hwang et al. [21] model.

In this paper, a simple STM is proposed to simulate the load capacity and failure mode of fix-ended RC deep beams subjected to monotonic and cyclic loads. Five experimental tests were conducted to study the nonlinear response these beams subjected to monotonic and cyclic loads. The proposed model was validated against 5 experimental tests of this paper and 31 additional tests. The results show the proposed STM can accurately predict the failure modes and ultimate load capacity of fix-ended RC deep beams subjected to monotonic and cyclic loads.

## 2. RESEARCH SIGNIFICANCE

Over 70 published papers in past decades [23] have focused on RC deep beams subjected to single curvature bending under point loads. Only a few papers focus on the behavior of fix-ended RC deep beams. In this paper, a novel STM which accounts for the concrete strut and web reinforcement is proposed. The newly proposed STM was calibrated using 5 experimental tests and

verified using an additional 31 independent experimental test data. The results show that the newly proposed curved STM can accurately predict the load capacity and failure mode of RC fix-ended deep beams subjected to monotonic and cyclic loads.

## 3. EXPERIMENTAL PROGRAM

In order to understand the nonlinear behavior of fix-ended RC deep beams subjected to cyclic and monotonic loads, five experimental tests were conducted.

**3. 1. Test Specimens** Table 1 shows the test specimens included in this study. The dimensions of all specimens are chosen according to the facility of structural laboratory and the reinforcement is selected according to the allowable range of ACI 318M-14 [13] considering easy for construction. Specimens SC1 to SC4 were subjected to cyclic load and Specimen SM was subjected to a monotonic load in the mid-span of the beams. SM and SC1 have the same property. SC2 has the same dimension as SC1, except 6 additional  $\phi 6$  bars were added in the web (as shown in Figure 1b). SC3 has the same dimension as SC1, except the longitudinal rebar was modified according to the information presented in Table 1. SC4 has the same dimension as SC3, except the yield, force of the web reinforcement was changed from 374 MPa to 242 MPa.

Table 2 shows the yielding stress of all reinforcements that are used in tested specimens. Figure 1 shows the overall dimensions and the reinforcement details for all specimens listed in Table 1. All beams had the same total length ( $L = 2260$  mm), clear span ( $L_n = 1680$  mm), width ( $b = 75$  mm) and depth ( $H = 600$  mm).

**TABLE 1.** Property of the fixed-end RC deep beams tested

Specimen	$f_c$ (MPa)	Main bars		Web bars		loading
		Top	Bot	Hor.	Ver.	
SM	36.6	2T20	2T16	10 $\phi 6$	34 $\phi 6$	Monotonic
SC1	37.2	2T20	2T16	10 $\phi 6$	46 $\phi 6$	Cyclic
SC2	35.2	2T20	2T16	10 $\phi 6$	34 $\phi 6$	Cyclic
SC3	33.3	2T12	2T12	10 $\phi 6$	34 $\phi 6$	Cyclic
SC4	35.2	2T12	2T12	10 $\phi 6$	34 $\phi 6$	Cyclic

**TABLE 2.** Material property of reinforcements

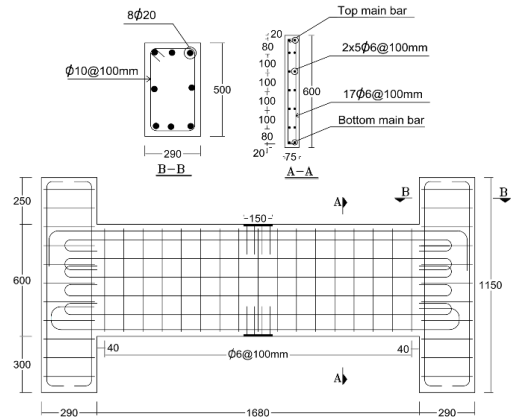
Reinforcement	Yielding stress (MPa)
T20	556
T16	510
T12	480
$\phi 6$ for oter specimens	374
$\phi 6$ for SC4	242

The main parameters investigated in this study were the amount and property of the web and longitudinal reinforcements, and the effect of the applied loads (cyclic or monotonic).

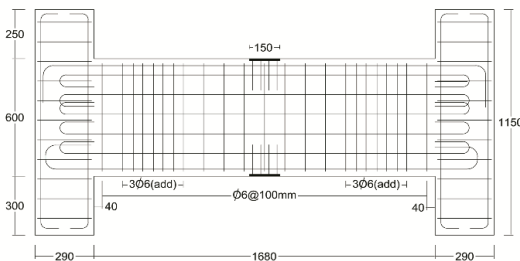
The ends of the RC fix-ended deep beams were constrained using end blocks. The dimensions of end blocks are 290×500 mm in cross section and 1150 mm in length. The reinforcements of the end blocks were capacity designed to ensure the deformation will concentrate within the RC fix-ended deep beams [24].

To avoid the stress concentration under the applied loads, two 10 mm thickness steel plates with a dimension of 150×75 mm size were added at the top and bottom of RC fix-ended deep beams at the location of the applied load. To anchor these plates, 8 (grade)  $\phi$ 10 bars with development length of 150mm were placed at the end of each plate. All the longitudinal reinforcing bars were extended to the full length and depth of the beam to ensure sufficient anchorage.

The concrete cover to the center of the main longitudinal bars was 30 mm, while the clear cover to the face of the stirrups was 20 mm. The vertical web reinforcement consisted of  $\phi$ 6@100mm distributed uniformly along the length of the RC fix-ended deep beams. The concrete compressive strength of each specimen was obtained from the cylinder test. Table 1 shows the property of concrete and reinforcements of all specimens.



(a) Dimension for Specimen SM, SC1, SC3, and SC4



(b) Dimension for Specimen SC2

Figure 1. Schematic view of the fix-ended RC deep beams

3. 2. Test Setup

The experimental tests have been done by using the frame reaction as shown in Figure 2. This frame has enough rigidity for supporting the end blocks of deep beams.

The experimental setup is shown in Figure 3. The setup consists of a frame reaction which connected the specimen as fix-ended using sixteen M27 grade A325 bolts at each end. The bolts were tightened to ensure the ends of the specimen do not slip.

The loading was provided by 2 static hydraulic actuators each with a tension and compression capacities of 1500 kN. Two high capacity load cells were added to the tip of the actuator to measure the force applied. The displacements were measured using five Linear Variable Differential Transducers (LVDT) as shown in Figure 3. Two LVDTs were utilized to measure the deformation of RC fix-ended deep beam at the mid span. Two additional LVDTs were utilized to measure the vertical deformation of the RC fix-ended deep beams at a distance of 500 mm from the end blocks. Lastly, a LVDT was used to measure the out-of-plan deformation beams at a distance of 700 mm from the end blocks. The cracks pattern at the end of each load step of were clearly marked and documented.



Figure 2. View of frame reaction of experimental tests

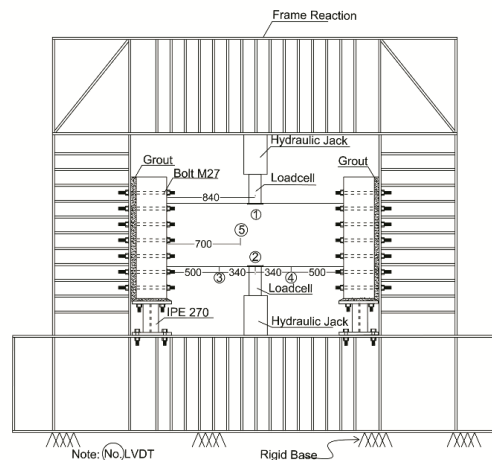


Figure 3. Schematic view of typical set-up equipment (all unit in mm)

**3. 3. Load Pattern** In this research, the loading protocol as presented in ATC-24 [25] was adopted. The loading (deformation) history consists of increasing cycles (multiple step test) as presented in Figure 4.

According to this algorithm, at first step, the displacement was selected to be 0.4 mm, at each amplitude three cycles were applied. After the first set of cycles, the amplitude of the loading then increased by 0.4 mm until  $\Delta$  reached 1.2 mm. After that, the amplitude was increased by 1.2 mm for three cycles of loading until the amplitude reached 3.6 mm. After that, the amplitude was increased by 1.2 but with 2 cycles until the capacity of the RC fix-ended deep beams reduced to 60% of the peak capacity.

As for the monotonic load, a small increment (1/10mm) was used to obtain the force-deformation relationship until the capacity of the RC fix-ended deep beams reduced to 60% of the peak capacity.

#### 4. EXPERIMENTAL RESULTS AND DISCUSSIONS

In this study, five fix-ended RC deep beams were tested under cyclic and monotonic load. The first diagonal crack in all of the test specimens was started at 20- 30% of the failure load as presented in Table 2. The diagonal crack occurred suddenly at the about mid-depth of the beam between the load point and the support in the second cycle of load step. After increasing load in the next steps, the length and width of the first crack increased and more diagonal and flexural cracks developed. In all beams under cyclic load, the crack patterns were similar in both side of loading point from top and bottom of the beams. In the last specimen, SM the crack pattern is similar other beams cracks just obtained from top loading.

Most of the major cracks in all specimens are parallel to diagonal cracks that shows the failure of these beams, are shear mode. It should be mentioned in some cases the top longitude rebar maybe yielded and the beam will be failed in flexural plus shear mode, and some of the cracks also occurred at the connection of the beam to the column.

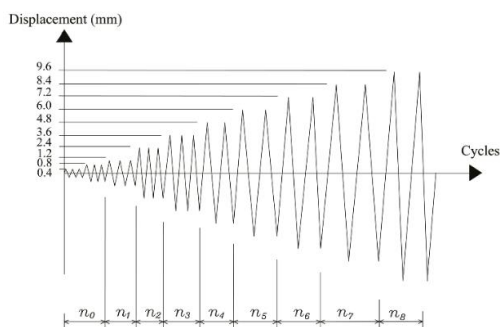


Figure 4. Loading history

All of the tested specimens in the present study have enough longitudinal reinforcement and failure in flexural plus shear mode did not happen after loading reach to the ultimate capacity of the beam. With increasing the displacement in the specimen subjected to cyclic loading, in addition to increasing the crack width, the concrete of crack crossed are is crashed and the cavity will be created. But, under monotonic loading, only the width of the crack will be increased. The test procedure was terminated when the bearing capacity is reduced to 60% of the peak capacity in all specimens except SC2; that was failed in bearing mode. Table 3 shows the summary of the experimental results.

According to the evidence of experimental tests, all the specimens' failure is the same in shear mode except the specimen SC2 that the concrete crashed under an applied load and failed in bearing mode.

The main cause of failure in all specimen was some major diagonal crack started that crossed each other at the mid depth of beams and extended along the distance between the edge of the load and intermediate support plates as shown in Figure 5 (SC1, SC3, and SC4). The failure, concrete crushing occurred at the cross of diagonal cracks in the cyclic loading. In the specimen SM, the diagonal cracks destroyed the concrete struts and the shear mechanism occurs under monotonic load (Figure 6). Also according to the results in Table 3, the capacity of fix-ended RC deep beams subjected to cyclic load is not a significant difference in comparing with the same beam subjected to a monotonic load. This little difference in capacity occurred because of changing in softening of the concrete strut with more cracks due to cyclic loading.

The specimen SC2 in Figure 5(b) again is subjected to cyclic loading and the first diagonal crack occurred at the force of 125 kN. In the reversed cycle, the diagonal crack occurred when the load reaches to 134 kN. With increasing loading, the new cracks occurred and extended the existing cracked, but since the stirrup increase, the capacity of beam increased significantly, so the beam failed locally under bearing plate in 549 kN and in reverse loading bearing fail occurred in 527 kN.

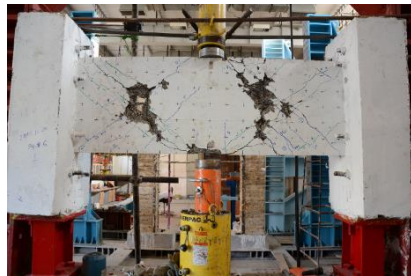
TABLE 3. Summary of experimental results

Specimen	1 <sup>st</sup> diagonal cracking load, kN (% of failure load)		Failure load, (kN)		Failure mode
	Top	Bot	Top	Bot	
SM	108(21%)	---	511	--	Shear
SC1	137(23%)	130(26%)	510	501	Shear
SC2	125(23%)	134(25%)	549	527	Bearing
SC3	118(25%)	117(25%)	483	472	Shear
SC4	124(30%)	127(30%)	421	418	Shear

The specimen SC3 in Figure 5(c) is subjected to cyclic loading and first diagonal crack occurred same as other specimens in 118 and 117 kN from the top and bottom loadings, respectively. Finally, the maximum bearing loads of this beam were 483 and 472 kN from top and bottom, respectively.

The specimen SC4 in Figure 5(d) is subjected to cyclic loading and the first diagonal crack occurred in 124 and 127 kN from the top and bottom loadings, respectively. The maximum bearing loads of this beam were 421 and 418 kN from top and bottom, respectively.

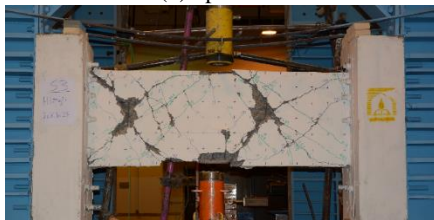
Figure 6 shows the beam SM is subjected to a monotonic load, the first diagonal crack occurred at 108 kN. As the loading increased, new cracks occurred and existing cracks extended. Finally, the maximum bearing load of this beam was 511 kN.



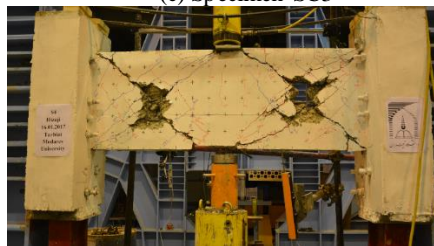
(a) Specimen SC1



(b) Specimen SC2



(c) Specimen SC3



(d) Specimen SC4

**Figure 5.** Crack propagation and failure modes of tested beams under cyclic load.

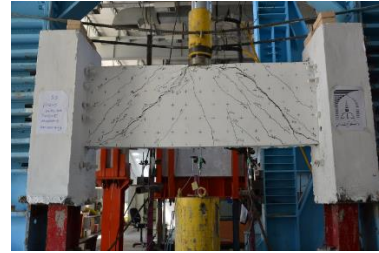


**Figure 6.** Crack propagation and failure mode of tested beams under monotonic load

## 5. STRUT AND TIE MODEL

After the development of the cracking pattern in the beam, the steel bars are subjected to tension, and the concrete acts as a compressive strut, thus forming a strut-and-tie action. Shear failure of the beam occurs when the concentrated flow of stresses along the diagonal strut surpasses the compressive capacity of the cracked reinforced concrete in the panel. The influence of the softened effect on concrete is thus considered for concrete strength [29]. This model is called the softened strut-and-tie model since it considers the softening effect, which weakens the concrete strength.

Based on the experimental study presented in the previous session, a simple STM (Strut and Tie Model) of the fixed-ended RC deep beams subjected to monotonic and cyclic point loads at the middle of the span was developed. The developed model was calibrated using the experimental result presented in this paper. The main steps of the STM model for predicting the shear strength are described as below.

**5. 1. Describe the Model** The proposed STM model is used for finding detailed relations to predict the final loading and failure mode of fixed-end deep beams in a simple yet accurate way and without the need for sophisticated computer programming. In this model, at each side of the loading point, the main strut and a sub strut equivalent to beam vertical reinforcements are used.

Figure 7 shows the proposed STM model, which comprises the diagonal and vertical mechanisms.

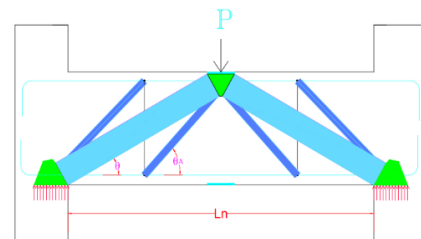


**Figure 7.** Schematic of Strut and tie model for fixed end deep beams

The diagonal mechanism is a diagonal compression concrete strut which is considered softening coefficient. The vertical mechanism consists of one vertical tie and two steep struts based on Lee and Hwang's studies [26]. The vertical tie is made up of vertical web reinforcements.

In this model, not all the vertical reinforcement of the beam participate in bearing the shear loading. Only the middle half and 50% of a quarter of the side reinforcements are effectively bearing the load. Therefore, the effective numbers of vertical web reinforcements of beam's half-span are obtained using Equation (1).

$$A_v = \rho_v \times b \times [(Ln - Lw)/4 + (Ln - Lw)/8] \quad (1)$$

Where  $\rho_v$  is the percentage of vertical web reinforcement,  $b$  is the thickness of beam,  $Ln$  and  $Lw$  are the spans of beam and width of loading plate respectively. The main strut is one of principle elements of proposed STM and to obtain the width of the strut, according to hyperbolic and linear equations from Equation (2) and the angle of strut, is obtain from Equation (3) are used.

$$T = ((Ln + Lw)H) / (6 \left( \left[ \frac{(Ln + Lw)}{2} \right]^2 + H^2 \right)^{0.5}) \quad (2)$$

$$\theta = \arctan \left( \frac{2d_h}{Ln - Lw} \right) \quad (3)$$

Here,  $T$  and  $\theta$  are width and angle of the main strut respectively.  $H$  is the high of the beam, and  $d_h$  is the effective beam height which, based on Bali and Hwang [27], is obtained by Equation (4).

$$d_h = H - (2 \times T / 3) \quad (4)$$

Since the vertical web reinforcements begin to yield upon beam failure in the final step of loading, the amount of final load that can be tolerated by the vertical web reinforcements is obtained using Equation (5)

$$P_v = A_v \times F_{yv} \quad (5)$$

Here,  $F_{yv}$  is the yielding stress and  $P_v$  is yielding force of the vertical web reinforcement. Given the loading tolerated by the web reinforcement, the bond load from the substrut is obtained from Equation (6).

$$F_{Bond} = P_v / \tan \theta_A \quad (6)$$

where  $F_{Bond}$  is a bond force of longitude top bars and  $\theta_A$  is the angle of sub strut obtained from Equation (7)

$$\theta_A = \arctan \left( \frac{4d_h}{Ln - Lw} \right) \quad (7)$$

If the bound force ( $F_{Bond}$ ) is less than the yield force of the longitudinal reinforcement ( $A_{S_{Top}} F_{yT}$ ), then the fix ended RC deep beam will fail in shear mode. Otherwise, fix ended RC deep beam will fail through a combination of flexural and shear mode and the slip- deflection of longitude bar will occur in concrete. We take the bond force equal to the yielding load of upper longitudinal reinforcement and then correct the tolerable loading on vertical reinforcement. Finally, the tolerable loading by

the vertical reinforcement,  $P_v$  is obtained by Equation (8).

$$P_v = \text{Min} [(A_v \times F_{yv}), (A_{S_{Top}} \times F_{yT} \times \tan \theta_A)] \quad (8)$$

where  $A_{S_{Top}}$  and  $F_{yT}$  are the amount and yielding stress of top reinforcements respectively. Next, the tolerable loading by the main strut,  $P_{Strut}$  is calculated using Equation (9).

$$P_{Strut} = f_{cd} \times b \times T \times \sin \theta \quad (9)$$

$f_{cd}$  is the effective compressive strength of the strut that can be calculated using Equation (10) as suggested by Hwang and Li [28].

$$f_{cd} = \xi f_c' \quad (10)$$

$$\xi = 3.35 / \sqrt{f_c'} \leq 0.52 \quad (11)$$

Here,  $f_c'$  is the compressive strength beam concrete and  $\xi$  is the concrete softening coefficient. At the end, the beam capacity is obtained using Equation (12).

$$P_{stm} = 2 \times (P_{Strut} + P_v) \quad (12)$$

## 5. 2. Procedure of Method

Figure 8 shows the flow chart for using the proposed STM. The procedure of STM is explain briefly as following:

Step 1: Specified the material (concrete and steel) and geometry properties of the fix-ended RC deep beams.

Step 2: Calculate the effective vertical web reinforcement area from Equation (1).

Step 3: Calculate the width and angle of the main strut from Equations (2) and (3).

Step 4: Check the bond force (Equation (6)) with the yield forces of the longitudinal rebars ( $A_{S_{Top}} F_{yT}$ ). If the bond force is less than the yield forces of the longitudinal rebar, the failure mode is a shear failure. If the bond force is greater than the yield forces of the longitudinal rebar, the failure mode is a shear-flexural failure

Step 5: Calculate the force of vertical web reinforcement from Equation (8).

Step 6: Calculate the force of the main strut from Equation (9).

Step 7: Calculate the capacity of the fix-ended RC deep beam using Equation (12).

## 5. 3. Experimental Verification

Once the parameters for the proposed STM have been calibrated d by experimental tests. The model was used to simulate the load capacity and failure mode of 31 additional experimental tests. These experimental tests are including; Subedi and Arabzadeh [3] involving 16 fixed- end RC deep beams, three specimens of Kim et al. [29], Hidalgo et al. [30], and Yang et al. [31].

Table 4 shows the summary of the experimental tests included in this study. The simulated load capacity and experimentally measured capacity for the 31 experimental tests are plotted in Figure 9. The result

shows excellent agreement between the STM model and experimental results.

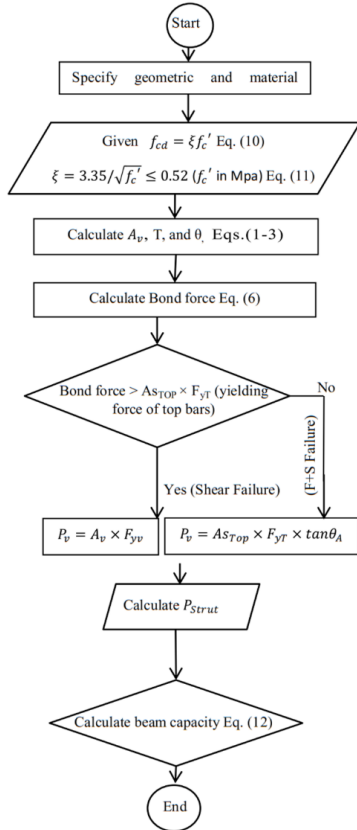


Figure 8. Flow chart of STM calculation procedure

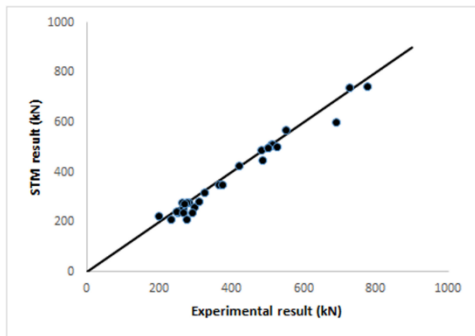


Figure 9. The experimental results against the STM results

The average ratio of beam capacity in the experimental results of this paper to STM results is 0.953. This is less than 5 % error. Also, these experimental tests involve different span to depth ratio, reinforcement, the compressive strength of concrete, and load algorithm are chosen from literature except author's experimental results. The second category of experimental results that were 16 fixed end RC deep beams have been tested under monotonic loading. In this group, the average strength ratio was 1.18 so this group was good agreement with the proposed STM model. The third category also was 3 fixed end deep beam that was tested under monotonic loading by Kim et al. [29] the AVG. of this group was 1.12. The next category of the experimental test was 11 double curvatures squat walls that are behavior like half of fixed end deep beams, so in this category, the shear capacity of squat walls can calculate as fixed end deep beams, but it will be divided by two. In this group, the AVG. was 0.93. The last specimen have been tested by Wei Yang et al. [31].

It should be noted the bearing failure mode must be prevented with suitable detailing around the loading area [32], so the results of beams the failure locally by bearing mode are excluded from statistic procedure in Table 4. According to the total average of the results, VAG is 1.06. Therefore, it obvious the propose STM model has good agreement with several types of experimental results (i.e. different dimension, reinforcement, and material property).

**5. 4. Advantages of the Proposed STM Model**

Compared to the existing methods, the benefits of the STM model can be summarized as follows:

- 1) High accuracy with percentage errors of about 5%.
- 2) Model simplicity and no computer requirement.
- 3) Prediction of beam failure mode by considering the amount of the main, top and bottom reinforcements and web reinforcements of the beam.
- 4) Consideration of the effect of concrete's compressive strength on its softening coefficient.
- 5) Consideration of the loading of beam's web reinforcements near the supports.

Derivation of the width of compressive strut independent from the beam's end wall as fixed-end deep beams are often connected to walls and the wall length should not affect the beam capacity.

TABLE 4. Experimental verification

Specimen	Dimension L <sub>n</sub> ×H×t (mm)	Concrete strength, f <sub>c</sub> ' (MPa)	Web reinforcements			Ultimate Load			Failure mode*		loading*
			ρ <sub>v</sub> (%)	ρ <sub>h</sub> (%)	F <sub>y</sub> (MPa)	Test (kN)	STM (kN)	V <sub>Test</sub> /V <sub>STM</sub>	Test	STM	
SC1	1680×600×75	37.2	0.87	0.87	374	510	542	0.94	S	S	C
SC2	1680×600×75	35.2	1.19	0.87	374	549	670	0.81	B	S	C
SC3	1680×600×75	33.3	0.87	0.87	374	483	515	0.94	S	S	C
SC4	1680×600×75	35.2	0.87	0.87	242	421	428	0.98	S	S	C
SM	1680×600×75	36.6	0.87	0.87	374	511	539	0.95	S	S	M

Subedi and Arabzadeh [3]	1B1	800×400×50	48.1	0.57	0.46	313	267	207	1.29	S+F	S+F	M	
	1B2	800×400×50	48.1	0.57	0.46	313	282	213	1.32	S	S	M	
	1B3	800×400×50	48.1	0.57	0.46	313	275	213	1.29	S	S	M	
	1B4	800×400×50	48.1	0.57	0.46	313	262	213	1.23	S	S	M	
	2B5	800×400×50	32.3	0.57	0.46	392	231	174	1.33	S+F	S+F	M	
	2B6	800×400×50	35.3	0.57	0.46	392	252	187	1.35	S+F	S	M	
	2B7	800×400×50	36.2	0.57	0.46	392	246	192	1.28	S	S	M	
	2B8	800×400×50	35.5	0.57	0.46	392	267	188	1.42	S	S	M	
	3B9	1680×600×75	34	0.76	0.66	403	512	501	1.02	S	S	M	
	3B10	1680×600×75	32.3	0.76	0.66	403	406	467	0.87	S	S+F	M	
	3B11	1680×600×75	33	0.76	0.66	403	525	495	1.06	S	S	M	
	3B12	1680×600×75	32.7	0.76	0.66	403	500	493	1.01	S	S	M	
	3B13	1680×600×75	32.3	0.76	0.66	403	502	491	1.02	S	S	M	
	4B14	1680×750×75	40.8	0.76	0.64	402	688	555	1.24	S+F	S+F	M	
	4B15	1680×750×83	36.8	0.69	0.58	402	725	649	1.12	B	S	M	
	4B16	1680×750×81	45.6	0.46	0.4	402	580	541	1.07	S	S	M	
Kim et al.	S-0.5-50	300×300×200	30.6	0.64	0	305	297	272	1.09	S	S	M	
	S-0.5-50	450×300×200	30.6	0.64	0	305	290	273	1.06	S	S	M	
	S-0.5-50	450×300×200	30.6	0.42	0	305	274	227	1.21	S	S	M	
Hidalgo et al. [31]	1	2000×1000×120	19.4	0.13	0.25	392	198	228	0.87	S	S	C	
	2	2000×1000×120	19.6	0.25	0.25	402	270	318	0.85	S	S	C	
	4	2000×1000×120	19.5	0.38	0.25	402	324	412	0.79	S	S	C	
	6	1800×1300×120	17.6	0.13	0.26	314	309	270	1.14	S	S	C	
	7	1800×1300×120	18.1	0.25	0.13	471	364	400	0.91	S	S	C	
	8	1800×1300×120	15.7	0.25	0.26	471	374	374	1.00	S	S	C	
	9	1800×1300×100	17.6	0.26	0.26	366	258	298	0.87	S	S	C	
	10	1800×1300×80	16.4	0.25	0.25	367	187	226	0.83	S	S	C	
	11	1400×1400×100	16.3	0.13	0.26	362	235	241	0.98	S	S	C	
	12	1400×1400×100	17	0.26	0.13	366	304	299	1.02	S	S	C	
	13	1400×1400×100	18.1	0.26	0.26	370	289	312	0.93	S	S	C	
	Yang et al. [32]	SW-1	700×700×100	53.73	0.283	0.32	270	330	321	1.03	S	S	C
	Avrage									1.06			

\* S: Shear failure. B: Bearing failure. S+F: Shear-flexure failure. C: Cyclic loading. M: Monotonic loading.

## 6. CONCLUSIONS

In this paper, five experimental tests of fix-ended RC deep beams were tested under monotonic and cyclic loads and proposed STM to calculate failure mode and load capacity of fix-ended RC deep beams. The following conclusions were drawn from the study presented:

- Based on the experimental tests presented, the load capacity of the fixed-end RC deep beams does not have a significant difference when subjected to cyclic and monotonic loads. This little difference in capacity occurred because of changing in softening

of the concrete strut with more cracks due to cyclic loading.

- According to the experimental result, first diagonal cracks have appeared 20 to 30 percent of beam capacity in all specimens and most of the cracks formed parallel to major diagonal cracks, that show these beams have shear behavior and the failure occur in shear mode in all specimens.
- The formations of cracks in the beams that are subjected to cyclic load are almost symmetrical and cross each other. This indicates the applied load has been equal of at top and bottom.



- The proposed STM considered bond action of main longitude reinforcements and determined the failure mode of deep beams.
- The proposed STM is compared with the measured ultimate capacity of 36 experimental tests with various types of parameters (i.e. deferent dimension, reinforcement, and material property), available in the literature, and the satisfactory correlation was found, furthermore the mean value of the results, AVG is 1.06. This indicates the good agreement between the STM model and experimental results

## 6. REFERENCES

1. Ashour, A.F. and Yang, K.-H., "Application of plasticity theory to reinforced concrete deep beams", *Magazine of Concrete Research*, (2008), 657-664.
2. Chae, H. and Yun, Y., "Strut-tie model for two-span continuous rc deep beams", *Computers and Concrete*, Vol. 16, No. 3, (2015), 357-380.
3. Subedi, N. and Arabzadeh, A., "Some experimental results for reinforced-concrete deep beams with fixed-end supports", *Structural Engineering*, Vol. 6, No. 2, (1994), 105-128.
4. Arabzadeh, A. and Hizaji, R., "Failure mechanism in fixed-ended reinforced concrete deep beams under cyclic load", *World Academy of Science, Engineering and Technology International Journal of Civil and Environmental Engineering*, Vol. 11, No. 4, (2017), 562 - 566.
5. Heidari, A. and Hashempour, M., "Investigation of mechanical properties of self compacting polymeric concrete with backpropagation network", *International Journal of Engineering, Transactions C: Aspects*, Vol. 31, No. 6, (2018), 903-909.
6. Alferjani, M., Samad, A.A., Elrawaff, B. and Mohamad, N., "Experimental and theoretical investigation on shear strengthening of rc precracked continuous t-beams using cfrp strips", *International Journal of Engineering-Transactions B: Applications*, Vol. 28, No. 5, (2015), 671-676.
7. Abdollahi, S., Ranjbar, M. and Ilbegyan, S., "Shear capacity of reinforced concrete flat slabs made with high-strength concrete: A numerical study of the effect of size, location, and shape of the opening", *International Journal of Engineering-Transactions B: Applications*, Vol. 30, No. 2, (2017), 162-170.
8. Heydari, M., Behnamfar, F. and Zibasokhan, H., "A macro-model for nonlinear analysis of 3d reinforced concrete shear walls", *International Journal of Engineering-Transactions B: Applications*, Vol. 31, No. 2, (2017), 220-227.
9. BS, B., "Structural use of concrete, part 1: Code of practice for design and construction", British Standards Institution, UK, (1997).
10. Association, C.S., "A23. 3-04: Design of concrete structures", Ontario, Canada, (2004).
11. Walraven, J.C. and Bigaj- van Vliet, A., "The 2010 fib model code for structural concrete: A new approach to structural engineering", *Structural Concrete*, Vol. 12, No. 3, (2011), 139-147.
12. Highway, A.A.o.S. and Officials, T., "Aashto lfrd bridge design specifications: Us customary units, American Association of State Highway and Transportation Officials, (2010).
13. Institute, A.C., "Building code requirements for structural concrete (aci 318-14): Commentary on building code requirements for structural concrete (aci 318r-14): An aci report, American Concrete Institute. ACI, (2014).
14. Hwang, S.-J., Lu, W.-Y. and Lee, H.-J., "Shear strength prediction for deep beams", *Structural Journal*, Vol. 97, No. 3, (2000), 367-376.
15. Yun, Y.M., "Nonlinear strut-tie model approach for structural concrete", *Structural Journal*, Vol. 97, No. 4, (2000), 581-590.
16. Park, J.-w. and Kuchma, D., "Strut-and-tie model analysis for strength prediction of deep beams", *ACI Structural Journal*, Vol. 104, No. 6, (2007), 581-590.
17. Chetchoisak, P., Teerawong, J., Yindeesuk, S. and Song, J., "New strut-and-tie-models for shear strength prediction and design of rc deep beams", *Computers and Concrete*, Vol. 14, No. 1, (2014), 19-40.
18. Alshegeir, A.A., "Analysis and design of disturbed regions with strut-tie models", (1994).
19. MacGregor, J.G., Wight, J.K., Teng, S. and Irawan, P., "Reinforced concrete: Mechanics and design, Prentice Hall Upper Saddle River, NJ, Vol. 3, (1997).
20. Arabzadeh, A., "Truss analogy for the analysis of reinforced concrete fixed-ended deep beams", in *The Second International Conference in Civil Engineering on Computer Applications, Research and Practice.*, (1996), 6-8.
21. Hwang, S.-J., Fang, W.-H., Lee, H.-J. and Yu, H.-W., "Analytical model for predicting shear strength of squat walls", *Journal of Structural Engineering*, Vol. 127, No. 1, (2001), 43-50.
22. Kassem, W., "Shear strength of squat walls: A strut-and-tie model and closed-form design formula", *Engineering Structures*, Vol. 84, (2015), 430-438.
23. Liu, J. and Mihaylov, B.I., "A comparative study of models for shear strength of reinforced concrete deep beams", *Engineering Structures*, Vol. 112, (2016), 81-89.
24. Arabzadeh, A. and Hizaji, R., "Effects of dimension and boundary condition of columns in rigidity of reinforced concrete deep beams", in *3rd international conference on Architecture, structure and civil engineering, Norway.*, (2016).
25. Krawinkler, H., "Guidelines for cyclic seismic testing of components of steel structures, Applied Technology Council, Vol. 24, (1992).
26. Hwang, S.-J. and Lee, H.-J., "Analytical model for predicting shear strengths of exterior reinforced concrete beam-column joints for seismic resistance", *ACI Structural Journal*, Vol. 96, (1999), 846-857.
27. Bali, I. and Hwang, S.-J., "Strength and deflection prediction of double-curvature reinforced concrete squat walls", *Structural Engineering and Mechanics*, Vol. 27, No. 4, (2007), 501-521.
28. Hwang, S.-J. and Lee, H.-J., "Strength prediction for discontinuity regions by softened strut-and-tie model", *Journal of Structural Engineering*, Vol. 128, No. 12, (2002), 1519-1526.
29. Kim, K.-H., Kim, W.-B., Kim, J.-M. and Kim, S.-W., "Composite strut and tie model for reinforced concrete deep beams", *Journal of Advanced Concrete Technology*, Vol. 7, No. 1, (2009), 97-109.
30. Hidalgo, P.A., Ledezma, C.A. and Jordan, R.M., "Seismic behavior of squat reinforced concrete shear walls", *Earthquake Spectra*, Vol. 18, No. 2, (2002), 287-308.
31. Yang, W., Zheng, S.-S., Zhang, D.-Y., Sun, L.-F. and Gan, C.-L., "Seismic behaviors of squat reinforced concrete shear walls under freeze-thaw cycles: A pilot experimental study", *Engineering Structures*, Vol. 124, (2016), 49-63.
32. Sharma, S.K., Kumar, P. and Roy, A., "Comparison of permeability and drying shrinkage of self compacting concrete admixed with wollastonite micro fiber and flyash", *International Journal of Engineering-Transactions B: Applications*, Vol. 30, No. 11, (2017), 1681-1690.

# A Simple Approach to Predict the Shear Capacity and Failure Mode of Fix-ended Reinforced Concrete Deep Beams based on Experimental Study

A. Arabzadeh, R. Hizaji

Department of Civil Engineering, Tarbiat Modares University, Tehran, Iran

## P A P E R I N F O

چکیده

### Paper history:

Received 07 January 2019

Received in revised form 23 January 2019

Accepted 07 March 2019

### Keywords:

Fix-ended Deep Beam

Strut and Tie Model

Shear Failure

Cyclic Load

تیرهای عمیق بتن مسلح عمدتاً در طراحی سازه‌هایی که در مسیر انتقال قائم بار، ناپیوستگی وجود دارد، استفاده می‌شود. با توجه به هندسه عمیق آنها، توزیع نیرو درون تیرهای عمیق بسیار متفاوت از تیرهای معمولی است. در چند دهه اخیر چندین مدل خرابایی برای تحلیل این تیرها ارائه شده است که اغلب آنها برای تیرهای عمیق دو سر ساده قابل استفاده است و برای تیرهای عمیق دو سر گیردار مناسب نیستند. در این مقاله، پنج تیر عمیق دو سر گیردار بتنی تحت بارهای یکنوا و چرخه‌ای آزمایش شده‌اند. همچنین، یک مدل خرابایی ساده برای پیش‌بینی ظرفیت باربری و حالت شکست این نوع تیرها ارائه شده است. مدل پیشنهاد شده دارای دستکهای فشاری اصلی و فرعی جهت شبیه‌سازی توزیع نیرو درون تیرهای عمیق دو سر گیردار می‌باشد. برای اعتبارسنجی مدل پیشنهادی علاوه بر نتایج نمونه‌های آزمایش شده در این مقاله، از نتایج ۳۱ آزمایش‌های موجود در ادبیات استفاده شده است. نتایج این آزمایش‌ها نشان می‌دهد که مدل جدید پیشنهاد شده می‌تواند ظرفیت بارگذاری و حالت شکست تیرهای عمیق دو سر گیردار را با دقت بسیار خوبی پیش‌بینی نماید.

doi: 10.5829/ije.2019.32.04a.03